Electronic Supplementary Material (ESI) for Journal of Materials Chemistry A.
This journal is © The Royal Society of Chemistry 2021

Supporting Information

Uniform Coverage of High-loading Sulfur on Cross-linked Carbon Nanofiber for High Reaction Kinetics in the Li-S Batteries with Low Electrolyte/Sulfur Ratio

Wenhao Wu, [a] Xiying Li, [b] Liangliang Liu, [a] Xuebing Zhu, [a] Zhijie Guo, [a] Wei Guo, [a] Qing Han, [a] Jinling He, * [a] Yong Zhao * [a]

[a] Key Lab for Special Functional Materials of Ministry of Education; National & Local Joint Engineering Research Center for High-efficiency Display and Lighting Technology; School of Materials Science and Engineering; Collaborative Innovation Center of Nano Functional Materials and Applications; Henan University, Kaifeng, 475004, P. R. China.

[b] College of Chemistry and Chemical Engineering, Henan University, Kaifeng, 475004, P. R. China.

*E-mail: hejinl@henu.edu.cn; zhaoyong@henu.edu.cn

Experimental Section

Materials

Phenol, 2-aminobenzimidazole, cetyl trimethyl ammonium bromide (CTAB), and nano titanium dioxide (TiO_2) were purchased from Macklin (Shanghai, China). Formaldehyde solution was purchased from Sinopharm Chemical Reagent Co. Ltd. Sublimed sulfur, carbon disulfide (CS_2), and lithium nitrate ($LiNO_3$) were purchased from Sigma Aldrich (Shanghai, China). Lithium sulfide (Li_2S) was purchased from Aladdin (Shanghai, China). 1,3-diamethoxyethane (DOL), 1,2-dimethyl ether (DME),

and lithium bis(trifluoromethanesulfonyl)imide (LiTFSI) were purchased from Suzhou Dodochem Co., Ltd, China. The water contents were below 15 ppm for solvents and 50 ppm for Li salt. Lithium-metal foil (thickness, 200 μm, 100 μm; diameter, 14 mm) was obtained from Shenzhen tianchenghe Technology Co., Ltd. All these materials were used without further purification.

Synthesis of Poly-NF@TiO_2 composite

Poly-NF was synthesized according to a previous report.[1] For the synthesis of Poly-NF@TiO_2, 0.44 g of phenol, 0.11 g of 2-aminobenzimidazole, 0.10 g TiO_2 and 0.30 g of CTAB were dissolved in 20 mL of deionized water. Then, the aqueous solution was placed in a thermostatic water bath operating at 60 °C under continuous stirring for 30 min followed by the addition of 0.9 mL of formaldehyde (37~40 wt%). After 1 h, the solution was transferred to a 50 mL Teflon-lined autoclave, which was placed in a thermostatic oven with a duration of 24 h at 180 °C. Then, the hydrothermal polymerization process was complete. Next, the foam product was immersed into deionized water for three times, followed by drying in a constant temperature drying oven for 12 h at 80 °C. Finally, we obtained the Poly-NF@TiO_2 foam. Based on this strategy, it is very easy to amplify synthesis production. In comparison, the synthesis procedure of Poly-NF was similar as that of Poly-NF@TiO_2 material, in which TiO_2 was not supported during the synthesis.

Synthesis of CNF TiO_2@CNF and TiC@CNF composite

Poly-NF was carbonized at 800 °C for 2 h under the pressure of ~0.05 MPa with a ramp rate of 3 °C min^{-1} and argon atmosphere to form the carbon nanofiber (CNF)

material. TiO_2@CNF material was prepared from Poly-NF@TiO_2 with the same treatment method to that of CNF (800 °C). Different from that of TiO_2@CNF material, the preparation of TiC@CNF was from a high annealing temperature of 1300 °C.

Preperation of Sulfur Loading Cathode

The sulfur loading in the carbon-based materials was carried out through the typical melt-diffusion method. A certain amount of sublimed sulfur was dissolved in CS_2 solvent. In the following step, the three (CNF, TiO_2@CNF, and TiC@CNF) carbon hosts were completely soaked in the CS_2 solution for 15 min, and then dried out at 60 °C for 12 h.

The S/CS_2 solution was dropped into the three (CNF, TiO_2@CNF, and TiC@CNF) carbon hosts, and then dried out at 60 °C for 12 h. Finally, the carbon composite covered with solid sulfur was placed in an autoclave and heated at 155 °C around the melting point of sulfur for 20 h to obtain the uniform carbon/sulfur electrodes. The sulfur loading for general electrodes was 3.1 mg cm^{-2}, while higher loadings (7 mg cm^{-2}, 12.5 mg cm^{-2}) were also prepared.

Characterizations

The morphology structure and elemental analysis of samples were characterized by a scanning electron microscope (SEM, Carl Zeiss, Gemini500) equipped with energy-dispersive X-ray (EDX) system and Transmission electron microscope (TEM, JEOL JEM-2100). The crystal structure of materials was characterized by X-ray diffractometer (XRD) with Cu Ka radiation (Bruker D8-Advanced). The Raman spectra were taken by Renishaw in Via with a 532.8-nm laser radiation. Nitrogen

adsorption/desorption measurements were conducted with Micromeritics ASAP2020. The mechanical testing of compressive was performed by using an electronic universal material testing machine (ITW Instron5965). The surface elemental compositions in the samples were measured by X-ray photoelectron spectroscopy (XPS, Kratos AXIS SUPRA). The TiO_2 content in TiO_2@CNF was investigated by thermogravimetric analysis (TGA, Mettler Toledo TGA/DSC3) at a temperature range of 25-800 °C with a ramp rate of 10 °C min^{-1} under air atmosphere. The sulfur content in these composites was investigated by thermogravimetric analysis at a temperature range of 25-600 °C with a ramp rate of 10 °C min^{-1} under argon atmosphere. UV-visible absorption spectra were measured by using UV-visible absorption spectrophotometry (PE Lambda 950).

Lithium Polysulfide Adsorption Test

0.5 M L^{-1} Li_2S_6 solution was prepared by dissolving 0.48 g sublimed sulfur and 0.138 g Li_2S in 6 mL of DOL and DME solvent (1:1 by volume) at 70 °C through continuous stirring. After 12 hours, a certain amount of Li_2S_6 solution (0.5 M L^{-1}) was diluted to 5 mM L^{-1}. The polysulfide adsorption test was carried out by adding different host materials (10 mg, respectively) to 2 ml Li_2S_6 solution (5 mM L^{-1}), and then the solution statically maintained for 6 h to observe color variation. The experiments were operated in an Ar-filled glove box.

Symmetric Cell Measurements

Symmetric cells were assembled using different host materials as working and counter electrodes, and PP membrane (Celgard 2400) as separator. The ether-based electrolyte containing 0.5 M Li_2S_6 was used. CR2025 coin cells were assembled in an

Ar-filled glove box. The CV curves were collected from -1.0 V to 1.0 V at a scan rate of 3 mV s^{-1} on a CHI 760E electrochemical workstation.

Cell Assembly and Electrochemical Measurements

Lithium-sulfur cells (CR2032) were assembled using different S/C free-standing materials as the cathodes and lithium foil as the anode in an Ar-filled glove box (< 0.1 ppm of O_2, < 0.1 ppm of H_2O). The electrolyte was composed of 1 M LiTFSI and a mixture of DOL and DME (1:1 by volume) with 2 wt% $LiNO_3$ additive. Celgard 2400 was used as the separator. The CT3001A cell test instruments (LAND Electronic Co., Ltd) were used for evaluating the cell performance between 1.7 and 2.8 V at room temperature (1 C=1675 mA g^{-1}). The CV curves were collected at the same potential range from 1.7 to 2.8 V with a scan rate of 0.1 mV s^{-1} by CHI 760E electrochemical workstation. Electrochemical impedance spectroscopy (EIS) tests were operated with an Autolab electrochemical workstation (Metrohm) in the frequency range of 100 kHz to 0.01 Hz and voltage amplitude of 5 mV.

Computational Section

To study adsorption process of Li_2S_x cluster on TiC (001) surface, plane-wave based spin-polarized DFT calculations were performed using the Vienna Ab initio Simulation Package. For the exchange-correlation energy, we employed the generalized-gradient approximation functional of Perdew-Burke-Ernzerhof (PBE). Electron–ion interactions were treated within the projector augmented wave framework. The convergence criteria for electronic and ionic optimization were respectively 10^{-5} eV and 0.01 eV/$Å^{-1}$, and the energy cutoff of plane wave basis set was

500 eV. The system energy calculations were performed at the 3 × 3 × 1 point, A 17.35 Å × 17.35 Å × 30 Å calculated surface supercell was used to eliminate the interaction between the neighboring cells, For Li_2S_x cluster, and the adsorption energies were calculated using:

$$E_{ad} = E_{surf+cluster} - E_{surf} - E_{cluster}$$

Where $E_{surf+cluster}$ is the total energy of the Li_2S_x cluster adsorbed on TiC (001) surface, E_{surf} is the total energy of TiC surface, and $E_{cluster}$ is the total energy of Li_2S_x cluster.

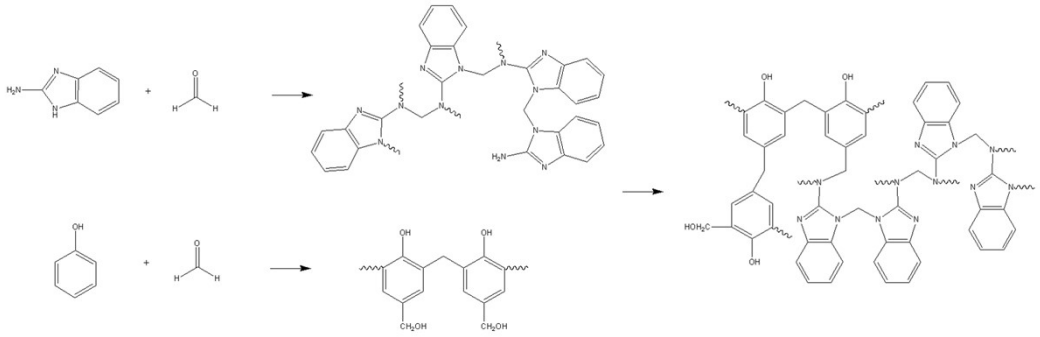

Figure S1. Schematic illustration of polymer production process.

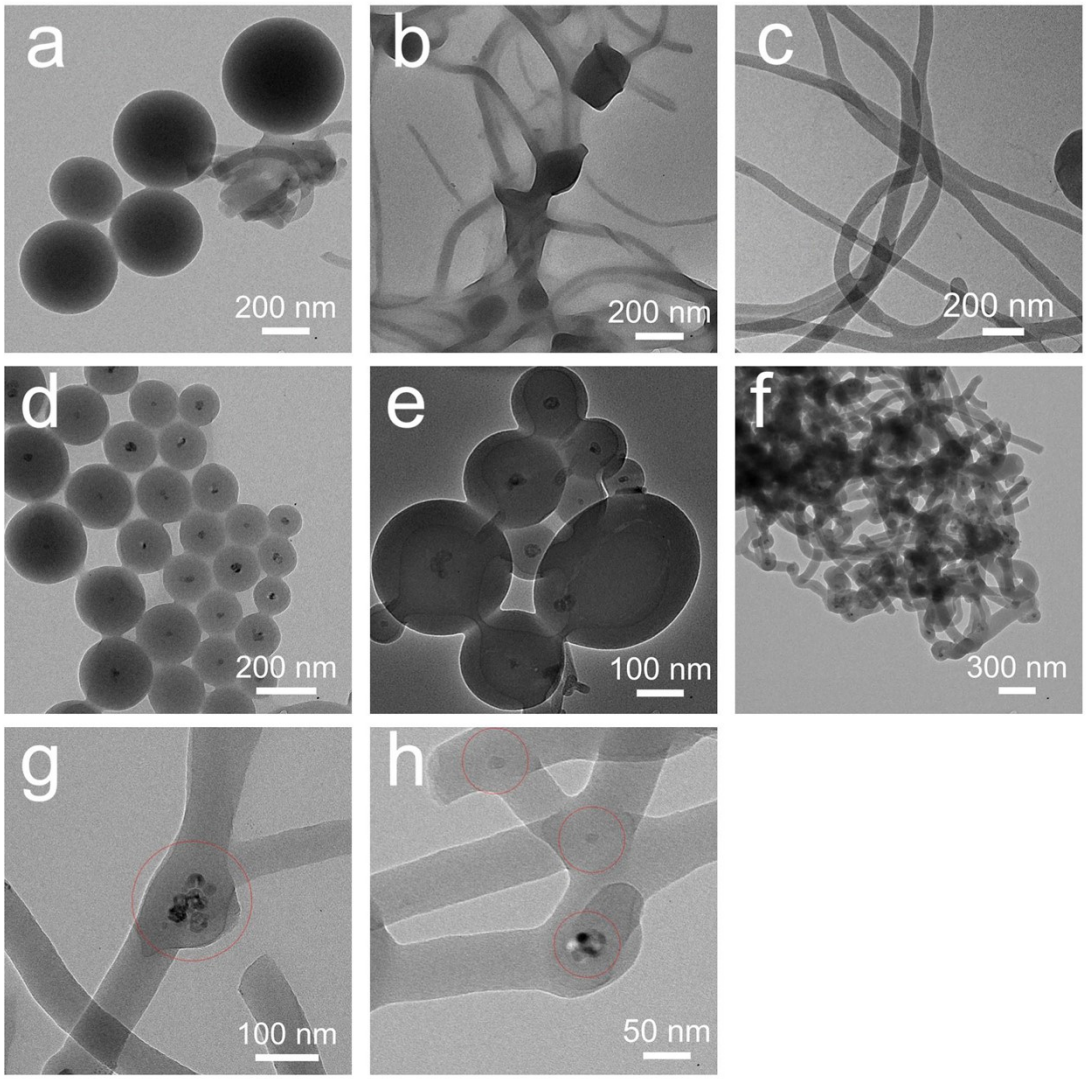

Figure S2. TEM images of (a, b, c) Poly-NF and (d, e, f, g, h) Poly-NF-TiO_2.

Note: The morphology in Figure S2a and S2b is Poly-NF precursor after 30 min and 2 h hydrothermal treatment, respectively. The morphology in Figure S2d and S2e is Poly-NF precursor after 30 min and 1 h hydrothermal treatment, respectively.

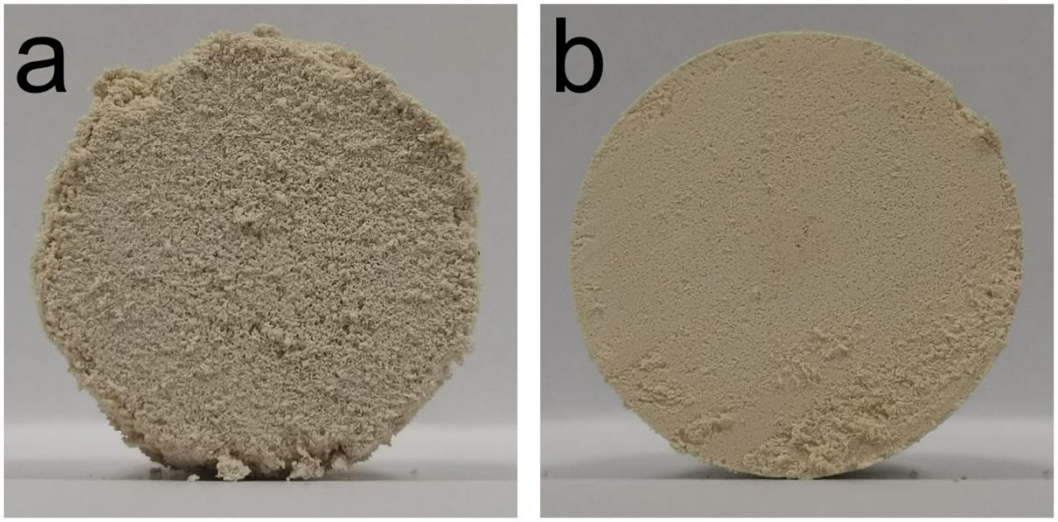

Figure S3. Optical photographs of a) Poly-NF, b) Poly-NF-TiO_2.

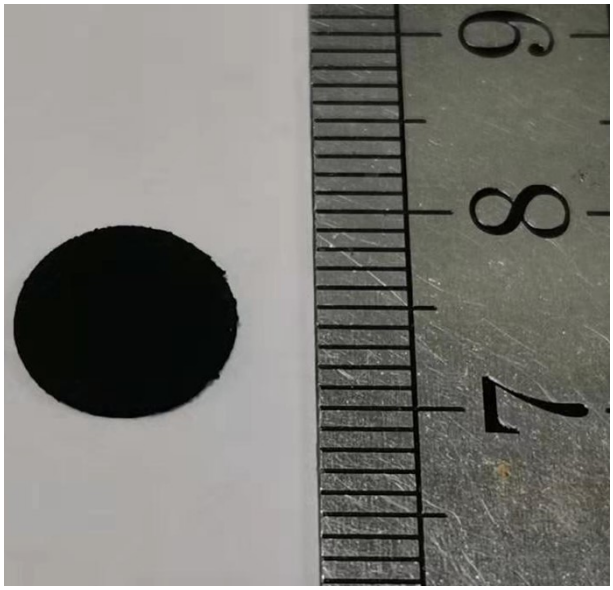

Figure S4. The size of collector host is 0.9 cm as the digital picture.

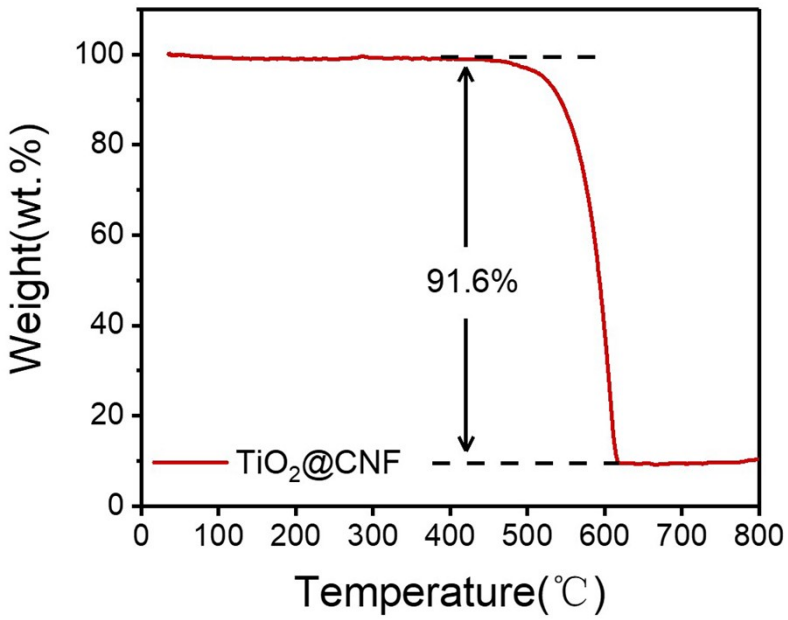

Figure S5. TGA curve of the TiO_2@CNF in the temperature range of 25-800 °C

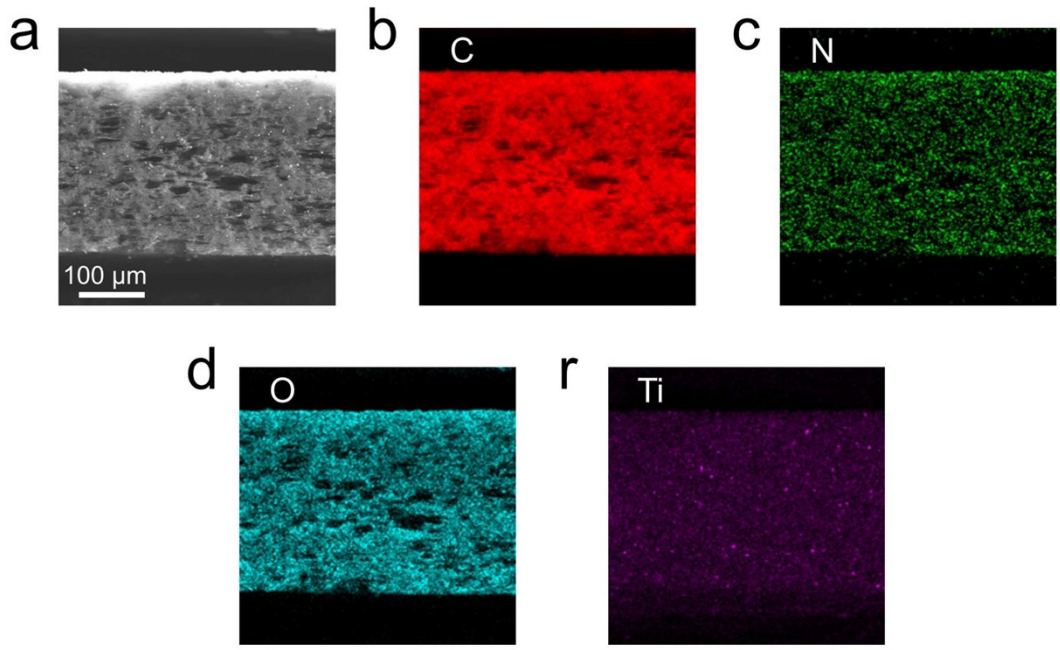

Figure S6. a) SEM image of TiO_2@CNF material and corresponding EDX elemental mappings of b) C, c) N, d) O, e) Ti.

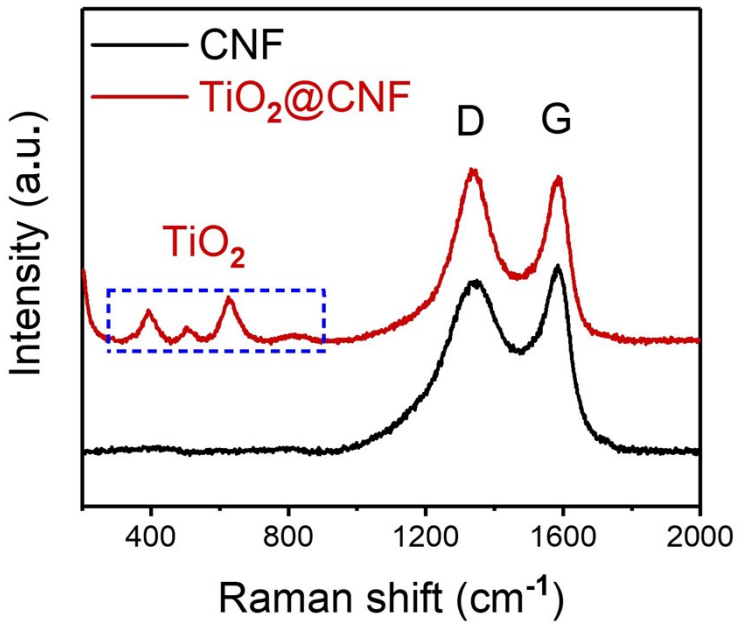

Figure S7. Raman spectra of CNFand TiO_2@CNF.

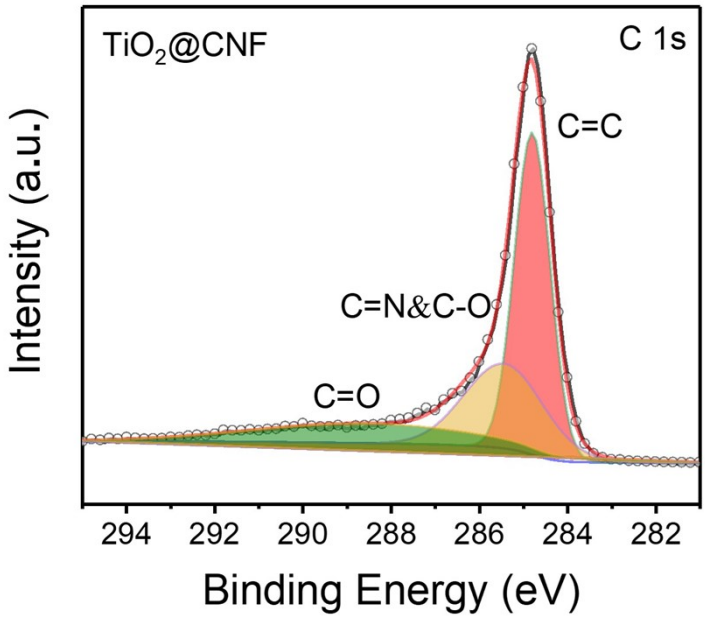

Figure S8. XPS C 1s spectra of TiO_2@CNF material.

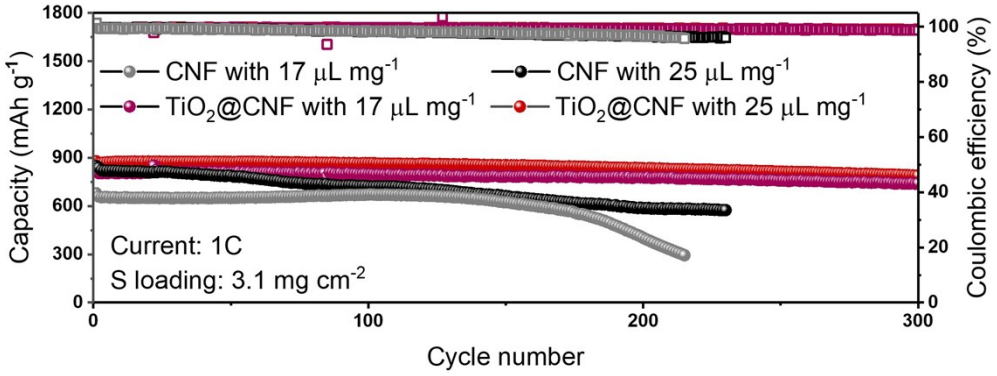

Figure S9. Long cycling performances of a) CNF/S and b) TiO_2@CNF/S at 1 C with different E/S ratios (sulfur loading of 3.1 mg cm^{-2}).

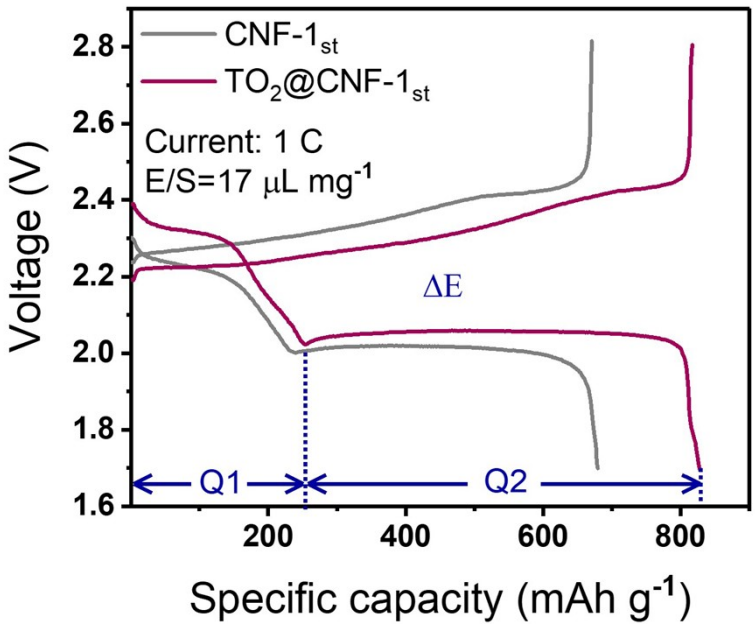

Figure S10. Contradistinction of cycle galvanostatic charge-discharge curves at 1 C.

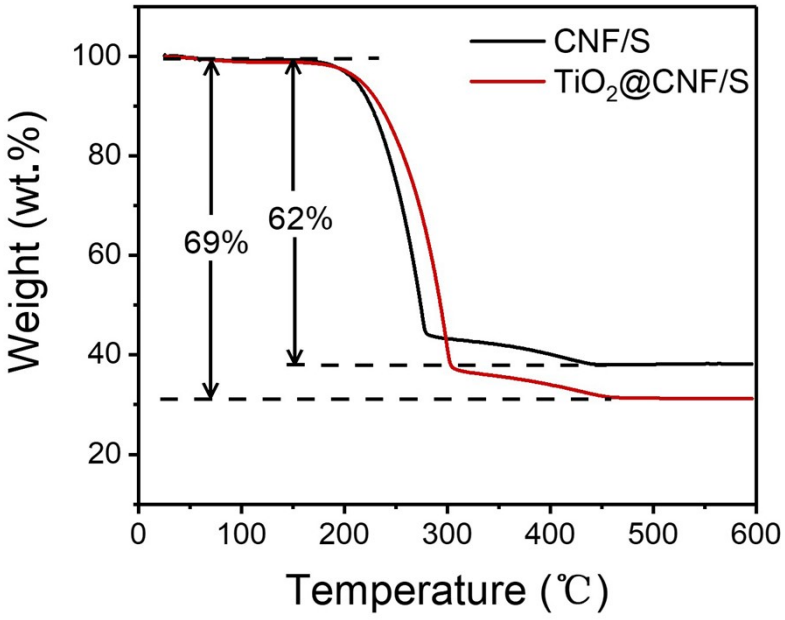

Figure S11. TGA curves of the CNF/S and TiO_2@CNF/S composite cathodes in the temperature range of 25-600 °C.

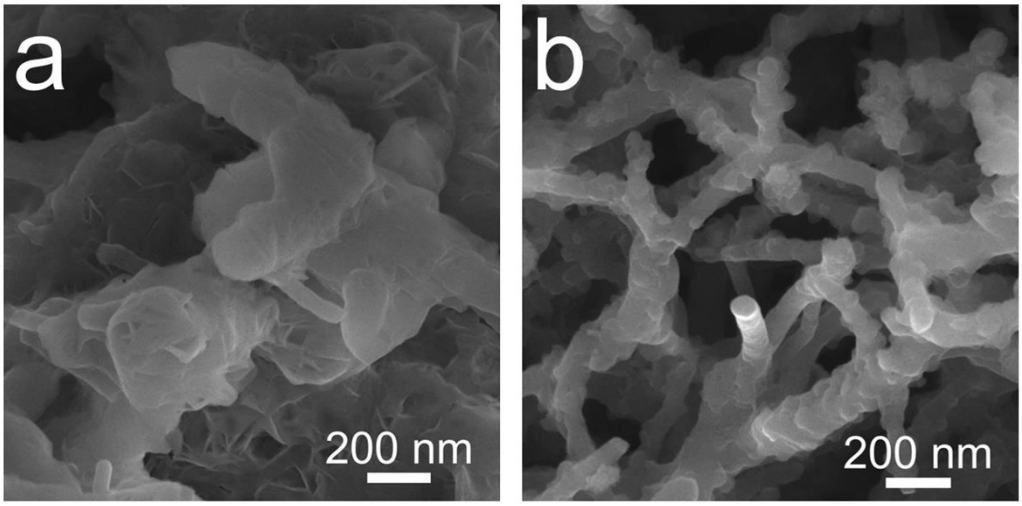

Figure S12. SEM images of a)CNF/Li_2S, and TiO_2@CNF/Li_2S.

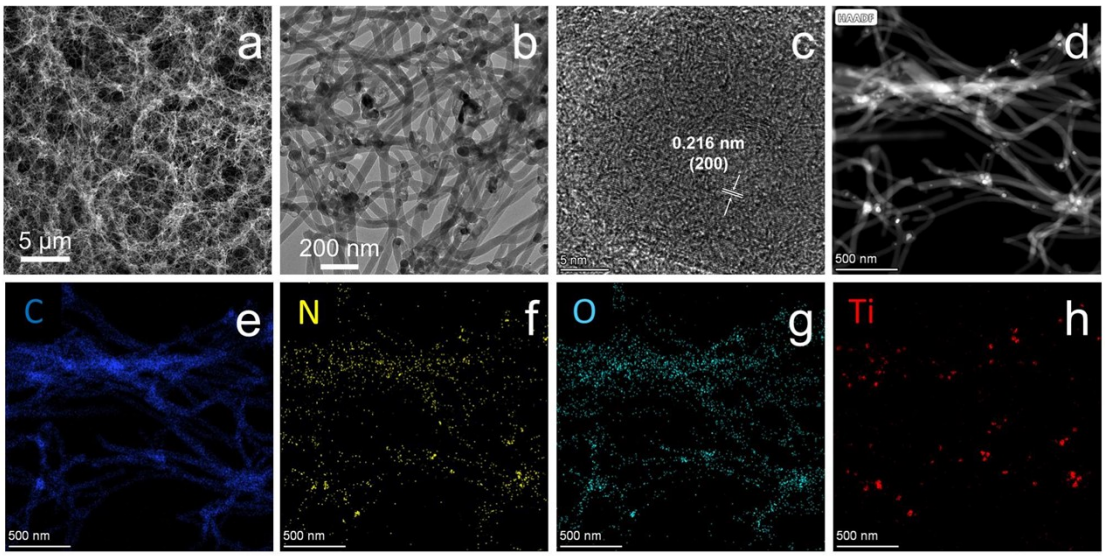

Figure S13. a) SEM image, b) TEM image and c) HRTEM image of TiC@CNF. d-h) HAADF-STEM image and the corresponding elemental mappings of TiC@CNF nanoflowers.

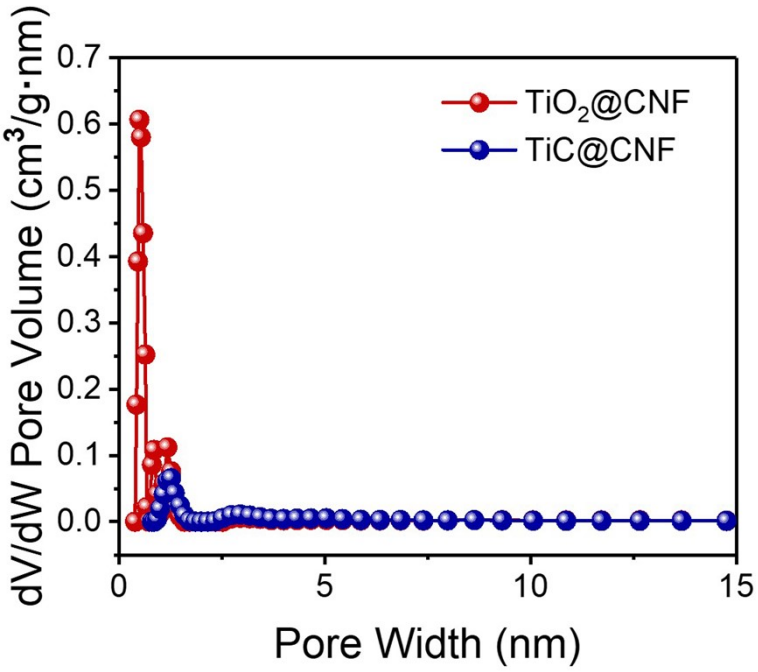

Figure S14. Pore size distributions of TiO_2@CNF and TiC@CNF materials.

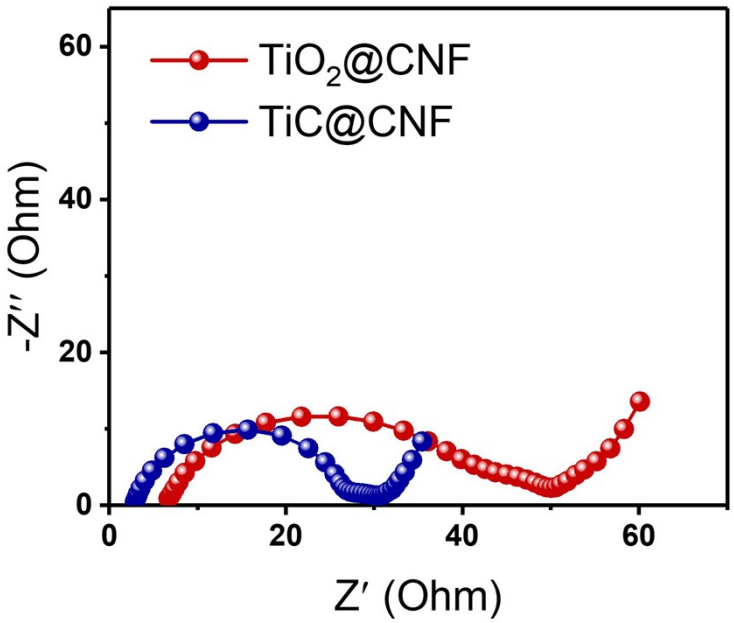

Figure S15. Electrochemical impedance spectra (EIS) of Li-S batteries with TiO_2@CNF/S and TiC@CNF/S cathodes

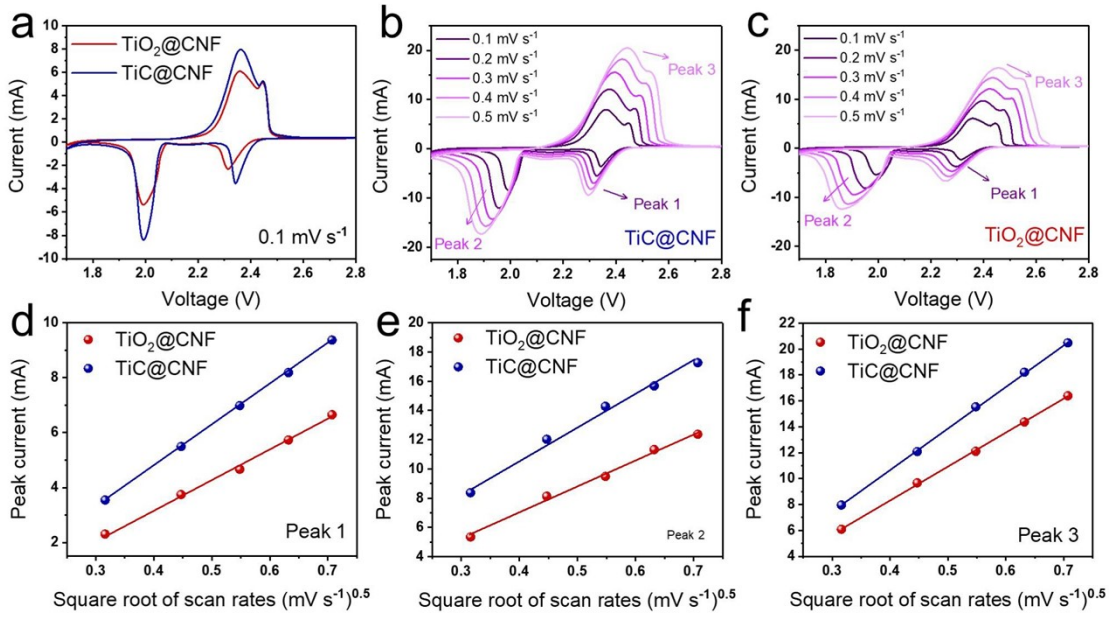

Figure S16. a) Cyclic voltammetric (CV) curves of Li-S coin cells with TiO_2@CNF/S and TiC@CNF/S cathodes at 0.1 mV s^{-1}. b) CV curves of TiC@CNF/S at different scan rate. c) CV curves of TiO_2@CNF/S at different scan rate. CV peak current for the d) frst cathodic reduction process (peak 1: $S_8 \rightarrow Li_2S_x$, $4 \leq x \leq 8$), e) second cathodic reduction process (peak 2: $Li_2S_x \rightarrow Li_2S_2/Li_2S$), and f) anodic oxidation process (peak 3: $Li_2S_2/Li_2S \rightarrow S_8$) versus the square root of the scan rates.

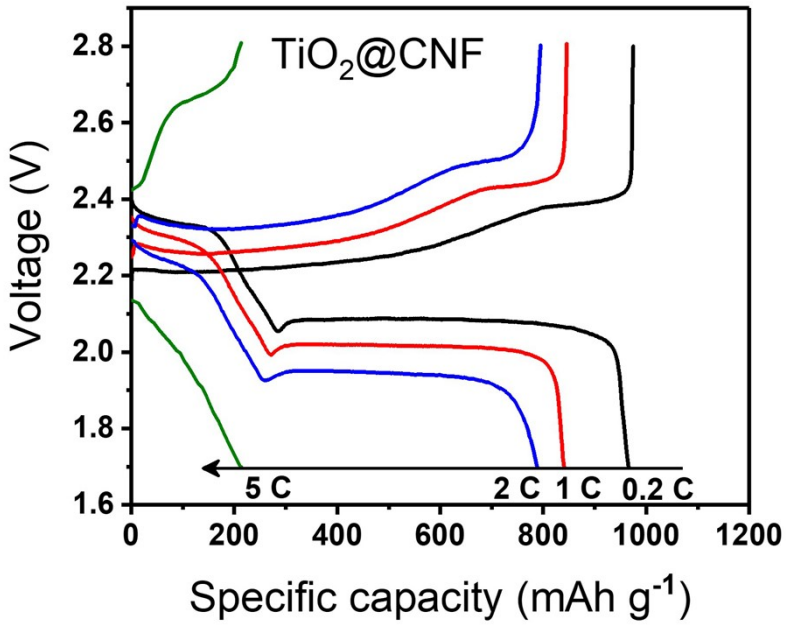

Figure S17. Galvanostatic discharge/charge voltage profles of TiO_2@CNF/S electrode under various current densities from 0.2 C to 5.0 C.

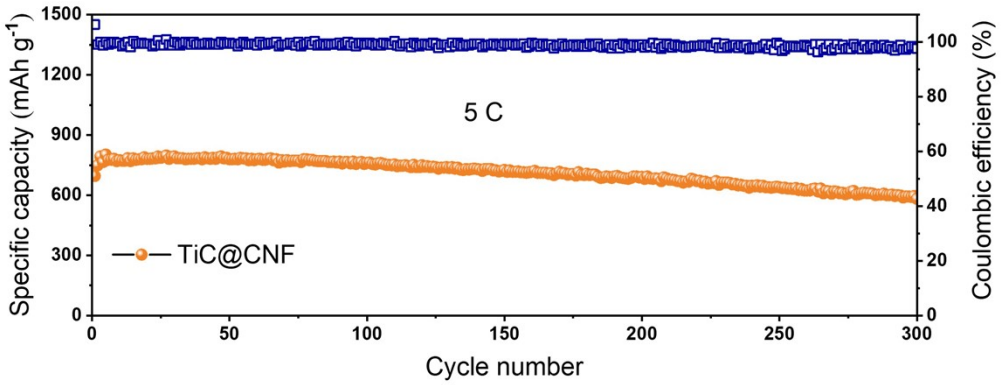

Figure S18. Long-term cycling test with TiC@CNF/S cathode at 5 C (the sulfur loading is 3.1 mg cm^{-2}).

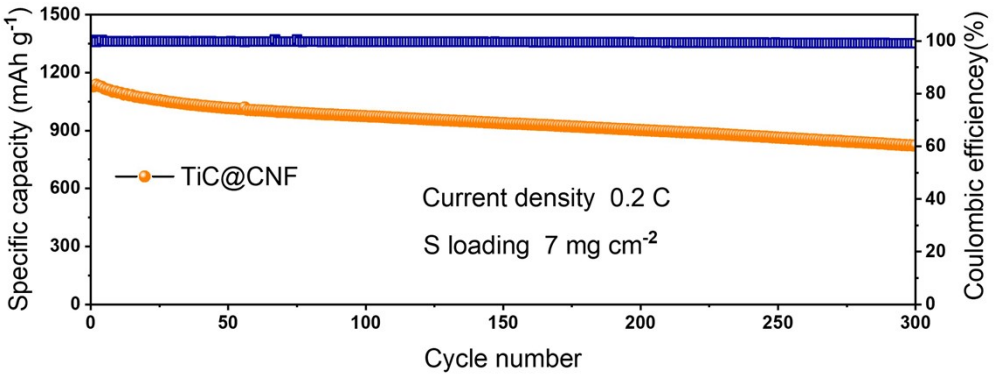

Figure S19. Long-term cycling test with TiC@CNF/S cathode at 0.2 C (the sulfur loading is 7.0 mg cm^{-2}).

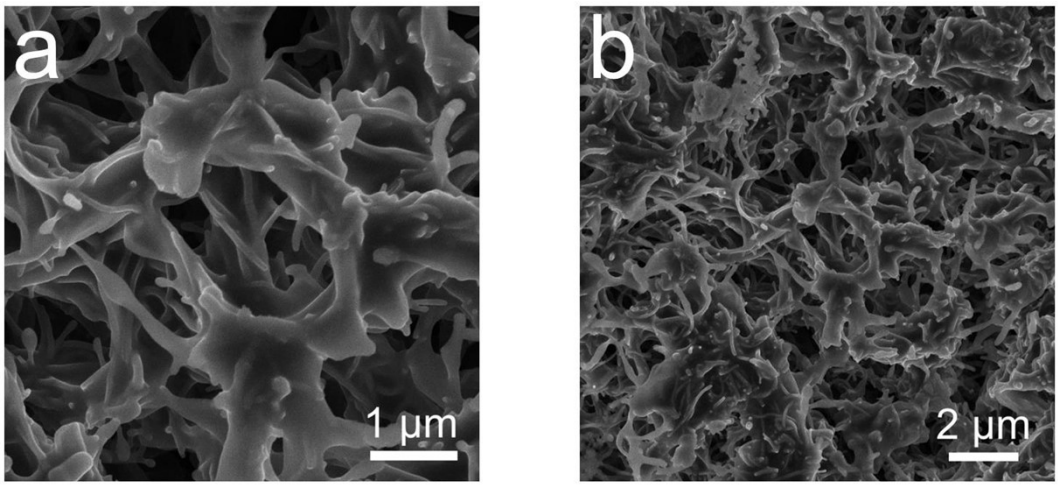

Figure S20. SEM images of the TiC@CNF/S surface (after discharge) at various scales, with sulfur loading of 12.5 mg cm^{-2}.

Table S1. Atomic and mass ratio of carbon, nitrogen, oxygen, and titanium elements from XPS test.

Element	Atomic %	wt %
C 1s	94.19	96.22
N 1s	0.72	1.16
O 1s	4.75	2.25
Ti 2p	0.34	0.37

Table S2. The results of D_{Li+} for the cathodic reduction process of TiO_2@CNF/S and TiC@CNF/S.

D_{Li+}（$cm^2\ s^{-1}$）	**Peak 1**	**Peak 2**	**Peak 3**
TiO_2@CNF	5.69×10^{-7}	1.49×10^{-6}	3.20×10^{-6}
TiC@CNF	1.02×10^{-6}	2.39×10^{-6}	4.72×10^{-6}

In the sulfur redox processes, the Li ion diffusion can be described by the classical Randle-Sevick equation: $Ip=(2.65\times10^5)\ n^{1/2}\ S\ D_{Li+}{}^{1/2}\ \Delta C_{Li}\ v^{1/2}$, where I_p (peak current) / $v^{1/2}$ (scan rate) should be positively correlated to the Li ion diffusion coefficient (D_{Li+}) in each step redox reaction due to the n (electrons number), S (geometric area of the cathode electrode), and ΔC_{Li} (Li ion concentration change in the electrochemical reaction) are constant.

Table S3. Comparison of cell performance with previously reported free-standing cathodes in LSBs

Cathode	Sulfur loading (mg cm^{-2})	Sulfur content	E/S ratio (μL mg^{-1})	Rate	Areal capacity after cycling (mAh cm^{-2})
CNT/NFC/S[2]	8.1	55%	30	0.25 C	4.7 (after 500 cycles)
TiO2@TiN/CNFs/S[3]	8	59%	-	3 mA cm^{-2}	6.41 (after 200 cycles)
Co-PCNF/S[4]	6	-	8.7	0.1 C	6.5 (after 50 cycles)
Co–TiO2-x/CNF/S[5]	7.8	-	3.8	0.1 C	4.8 (after 100 cycles)
S/PCNF/CNT[6]	12	62%	20	0.6 mA cm^{-2}	10.8 (after 50 cycles)
3DG/TM/S[7]	10	-	8	0.1 C	11.37 (after 200 cycles)
3D S/GCN[8]	5	82%	20	1 C	3.79 (after 150 cycles)
CNCF/S[9]	6.9	71%	-	0.2 C	5.5 (after 300 cycles)
VO2(P)-NCNT/S[10]	9.6	-	12.5	0.2 C	5.7 (after 200 cycles)
GF–rGO/S[11]	14.36	83%	34	0.2 C	6.3 (after 350 cycles)
ACImPPO/S[12]	9.1	40.6%	-	0.1 C	5.8 (after 200 cycles)
SWCNT/CNF/S[13]	16	60%	15	0.1 C	7.1 (after 100 cycles)
3DP@Li2S[14]	7	-	14.3	0.5 C	6.29 (after 100 cycles)
CC@CoP/C/S[15]	4.17	78%	30	0.1 C	3.07 (after 100 cycles)
CNF/LPS/CNT/Mo[16]	7.64	-	7.85	0.2 C	4.75 (after 100 cycles)
CNT foam/S[17]	19.1	79%	-	0.1 C	9 (after 100 cycles)
3D CNT foam[18]	7.1	66%	11	0.2 C	6.2 (after 150 cycles)
This work	**7** **12.5**	**69%** **82%**	**12** **6**	**0.2 C** **0.1 C**	**5.8 (after 300 cycles)** **9 (after 150 cycles)**

Supported References

1. X. Li, L. You, Y. Song, L. Gao, Y. Liu, W. Chen and L. Mao, *Langmuir*, 2019, **35**, 14902-14912.
2. M. Yu, J. Ma, M. Xie, H. Song, F. Tian, S. Xu, Y. Zhou, B. Li, D. Wu, H. Qiu and R. Wang, *Adv. Energy Mater.*, 2017, **7**, 1602347.
3. C. Qi, M. Cai, Z. Li, J. Jin, B. V. R. Chowdari, C. Chen and Z. Wen, *Chem. Eng. J.*, 2020, **399**, 125674.
4. T. Huang, Y. Sun, J. Wu, J. Jin, C. Wei, Z. Shi, M. Wang, J. Cai, X.-T. An, P. Wang, C. Su, Y.-y. Li and J. Sun, *ACS Nano*, 2021, DOI: 10.1021/acsnano.1c04642.
5. J. Wang, D. Luo, J. Li, Y. Zhang, Y. Zhao, G. Zhou, L. Shui, Z. Chen and X. Wang, *Nano Energy*, 2020, **78**, 105293.
6. Y.-Z. Zhang, Z. Zhang, S. Liu, G.-R. Li and X.-P. Gao, *ACS Appl. Mater. Inter.*, 2018, **10**, 8749-8757.
7. J. He, G. Hartmann, M. Lee, G. S. Hwang, Y. Chen and A. Manthiram, *Energy Environ. Sci.*, 2019, **12**, 344-350.
8. J. Zhang, J.-Y. Li, W.-P. Wang, X.-H. Zhang, X.-H. Tan, W.-G. Chu and Y.-G. Guo, *Adv. Energy Mater.*, 2018, **8**, 1702839.
9. Y. Liu, G. Li, Z. Chen and X. Peng, *J. Mater. Chem. A*, 2017, **5**, 9775-9784.
10. S. Wang, J. Liao, X. Yang, J. Liang, Q. Sun, J. Liang, F. Zhao, A. Koo, F. Kong, Y. Yao, X. Gao, M. Wu, S.-Z. Yang, R. Li and X. Sun, *Nano Energy*, 2019, **57**, 230-240.

11. G. Hu, C. Xu, Z. Sun, S. Wang, H.-M. Cheng, F. Li and W. Ren, *Adv. Mater.*, 2016, **28**, 1603-1609.

12. D. Guo, M. Li, M. N. Hedhili, V. Tung, Y. Li and Z. Lai, *Energy Storage Mater.*, 2020, **25**, 33-40.

13. C.-H. Chang, S.-H. Chung and A. Manthiram, *Mater. Horiz.*, 2017, **4**, 249-258.

14. L. Xue, L. Zeng, W. Kang, H. Chen, Y. Hu, Y. Li, W. Chen, T. Lei, Y. Yan, C. Yang, A. Hu, X. Wang, J. Xiong and C. Zhang, *Adv. Energy Mater.*, 2021, **11**, 2100420.

15. Z. Wang, J. Shen, J. Liu, X. Xu, Z. Liu, R. Hu, L. Yang, Y. Feng, J. Liu, Z. Shi, L. Ouyang, Y. Yu and M. Zhu, *Adv. Mater.*, 2019, **31**, 1902228.

16. Y. Li, C. Wang, W. Wang, A. Y. S. Eng, M. Wan, L. Fu, E. Mao, G. Li, J. Tang, Z. W. Seh and Y. Sun, *ACS Nano*, 2020, **14**, 1148-1157.

17. M. Li, R. Carter, A. Douglas, L. Oakes and C. L. Pint, *ACS Nano*, 2017, **11**, 4877-4884.

18. R. Ummethala, M. Fritzsche, T. Jaumann, J. Balach, S. Oswald, R. Nowak, N. Sobczak, I. Kaban, M. H. Rümmeli and L. Giebeler, *Energy Storage Mater.*, 2018, **10**, 206-215.